ACS NANO

ARTICLE

Bacterial Outer Membrane Porins as Electrostatic Nanosieves: Exploring Transport Rules of Small Polar Molecules

Harsha Bajaj,[†,⊥] Silvia Acosta Gutierrez,[‡,⊥] Igor Bodrenko,[‡] Giuliano Malloci,[‡] Mariano Andrea Scorciapino,[§] Mathias Winterhalter,[†] and Matteo Ceccarelli[*,‡]

[†]Jacobs University Bremen, Campus Ring 1, D-28759 Bremen, Germany
[‡]Department of Physics, University of Cagliari, 09124 Cagliari, Italy
[§]Department of Biomedical Sciences, University of Cagliari, 09124 Cagliari, Italy

Ⓢ *Supporting Information*

ABSTRACT: Transport of molecules through biological membranes is a fundamental process in biology, facilitated by selective channels and general pores. The architecture of some outer membrane pores in Gram-negative bacteria, common to other eukaryotic pores, suggests them as prototypes of electrostatically regulated nanosieve devices. In this study, we sensed the internal electrostatics of the two most abundant outer membrane channels of *Escherichia coli*, using norfloxacin as a dipolar probe in single molecule electrophysiology. The voltage dependence of the association rate constant of norfloxacin interacting with these nanochannels follows an exponential trend, unexpected for neutral molecules. We combined electrophysiology, channel mutagenesis, and enhanced sampling molecular dynamics simulations to explain this molecular mechanism. Voltage and temperature dependent ion current measurements allowed us to quantify the transversal electric field inside the channel as well as the distance where the applied potential drops. Finally, we proposed a general model for transport of polar molecules through these electrostatic nanosieves. Our model helps to further understand the basis for permeability in Gram-negative pathogens, contributing to fill in the innovation gap that has limited the discovery of effective antibiotics in the last 20 years.

KEYWORDS: *porins, transport, antibiotics, Gram-negative bacteria, single-molecule electrophysiology, molecular simulations, electric field*
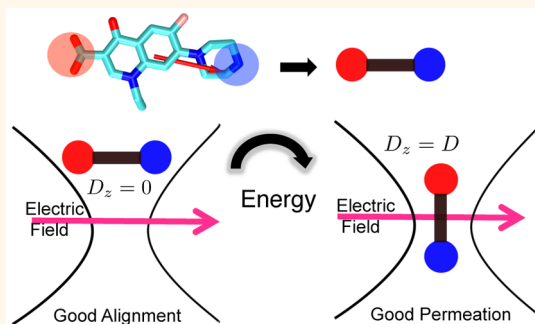
Transport of essential compounds like nutrients, vitamins, or even proteins through biological membranes is a fundamental process, often driven by diffusion.[1] Due to the hydrophobic nature of the membranes, polar compounds will likely use one or several membrane nanochannels as main path for overcoming the membrane barrier. In the case of Gram-negative bacteria, these channels, also called porins, are β-barrel transmembrane proteins constricted in the central region by the presence of an internal loop that hinders free diffusion. Other biological channels like the mitochondrial VDAC[2,3] or the CymA pore in *Klebsiella oxytoca*[4] share a similar architecture. In the *Escherichia coli* general porins OmpF/OmpC the constricted area, which is decorated with charged residues, has a double function: to preserve the permeability barrier of the outer membrane and to filter both desired and noxious polar molar molecules like nutrients and antibiotics, making them a suitable prototype for electrostatic nanosieve devices. In previous studies, these porins have been already recognized as nanodevices for ion-current

rectification[5] and for orientation-based filtering of small molecules,[6−8] e.g., aquaporins.[9,10] However, the molecular mechanism modulating passive transport of small polar molecules is still unknown.[11] Both the lack of knowledge on the physical/chemical rules for filtering and of robust methods to measure transport through bacterial membrane represent today a severe bottleneck in drug discovery.[12−15]

Nowadays, mass spectroscopic techniques are available to measure accumulation of molecules in relatively large compartments, whereas the small bacteria are still a challenge.[16] Intrinsic fluorescence has been used as a detection method to quantify both *in vitro*[17] and *in vivo*[18,19] the uptake across proteins, but unfortunately it is limited to only certain classes of molecules. Previous attempts have shed some light into

Experimental set-up
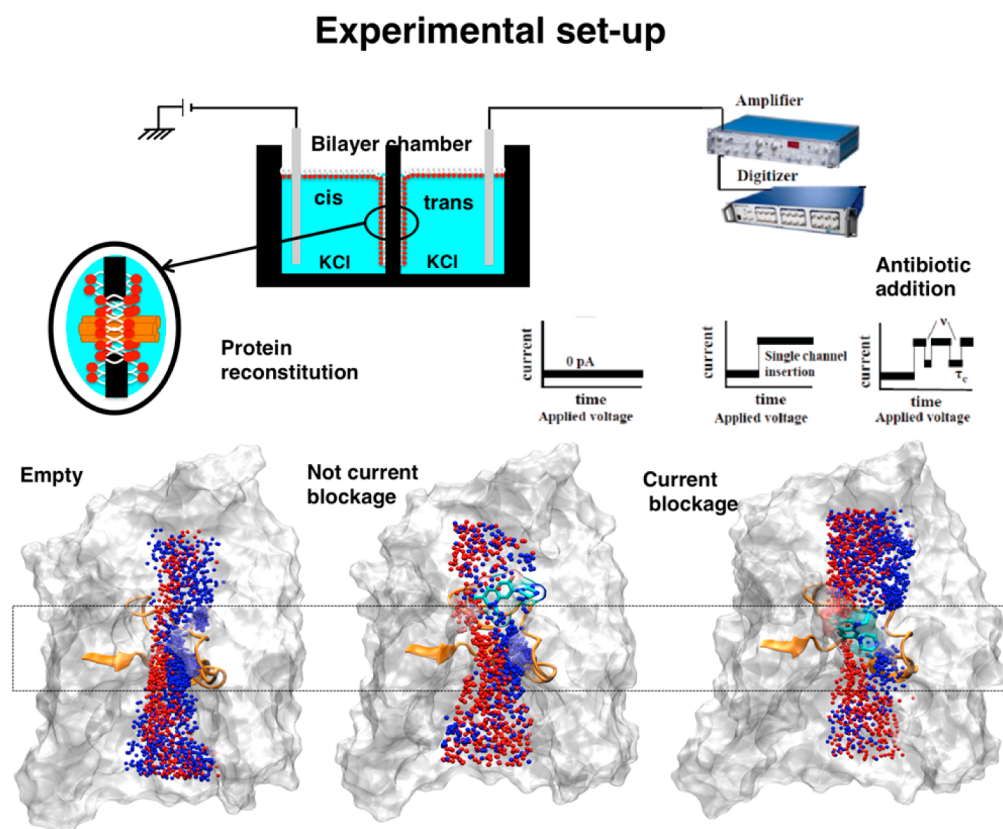
Figure 1. Top panel: Planar lipid bilayer electrophysiology experimental set up and molecule-channel interaction cartoon. Bottom panel: Protein channel is represented as Van der Walls surface in white; the pore-constricting loop is highlighted in orange and represented as new cartoon. Free-flowing ions (cations: blue; anions: red) are depicted as small spheres while the molecule is represented as licorice. When the channel is empty (left) ions freely diffuse generating the experimental current signal. In presence of a molecule, we can have interactions with the channel walls above the constricting loop without disturbing the ion pathways (center) or in contact with the constricting loop (right), in the latter case leading to the experimental current blockages.

molecule-channel interactions using electrophysiology combined with all atom modeling. In a number of cases, the penetration of antibiotics into the channel causes substantial flickering in the ion current.[20] In case of strong interactions current blockages can be used to propose a translocation model, though blockages themselves provide information on the interaction with the channel and only indirectly on the transport.[20] Nevertheless, application of an external electric potential can have an effect on the residence time that allows to clearly distinguish between translocation and repulsion of charged molecules.[20] Experiments of pulling charged polymers like DNA or proteins have been performed quite extensively in model pores to understand their translocation mechanism and for biosensing applications.[21,22] Charged molecules like peptides can be pulled through the pore[23] by applied electric potential, and neutral molecules may be dragged by electro-osmotic effect when ions diffuse through the charge selective pores.[24−26] However, in the case of transport across porins of small polar molecules, like nutrients or drugs, detailed voltage effects on the kinetics have not been reported so far.[27,28]

In this study, we revealed the rules behind transport of polar molecules by using OmpF and OmpC porins as prototypes. Unlike previous investigations, where ions were used to sense the internal electrostatics of channels,[29] here we used a rigid dipolar (zwitterionic) molecular probe, the norfloxacin antibiotic. In contrast with the linear signature of charged polymers pulling or electro-osmosis, we report here an unexpected strong

exponential voltage dependence of the kinetic rate constants of the antibiotic interacting with the pores.

By combining enhanced sampling molecular dynamics simulations with single-channel electrophysiology experiments on selected mutants, we propose a two-step kinetic model for the transport of polar molecules through the OmpF model pore. By using this simple model, we can estimate the transversal electric field in the narrowest region of the channel and quantify the distance where the applied potential drops, ultimately suggesting general rules for polar molecules transport across electrostatic nanosieves.

RESULTS

Experimental Results. Norfloxacin is present in a zwitterionic isoform at pH 7 with a large electric dipole moment, 44 D compared to its anionic (25 D) or cationic (27 D) forms (SI, Figure S1).[8] In order to investigate at a macroscopic time scale the interaction between norfloxacin and OmpF, we performed single-molecule electrophysiology experiments (Figure 1 as described in Materials and Methods Section) with single OmpF trimers reconstituted in planar lipid membranes. Upon addition of 100 μM norfloxacin to the cis (extracellular) side of the channel we observed well resolved full monomer blockages with a long average residence time, about 1.5 ms at −100 mV. In contrast, at +100 mV, we observed a significantly less number of events with lower average residence time, about 0.2 ms. On the other hand,
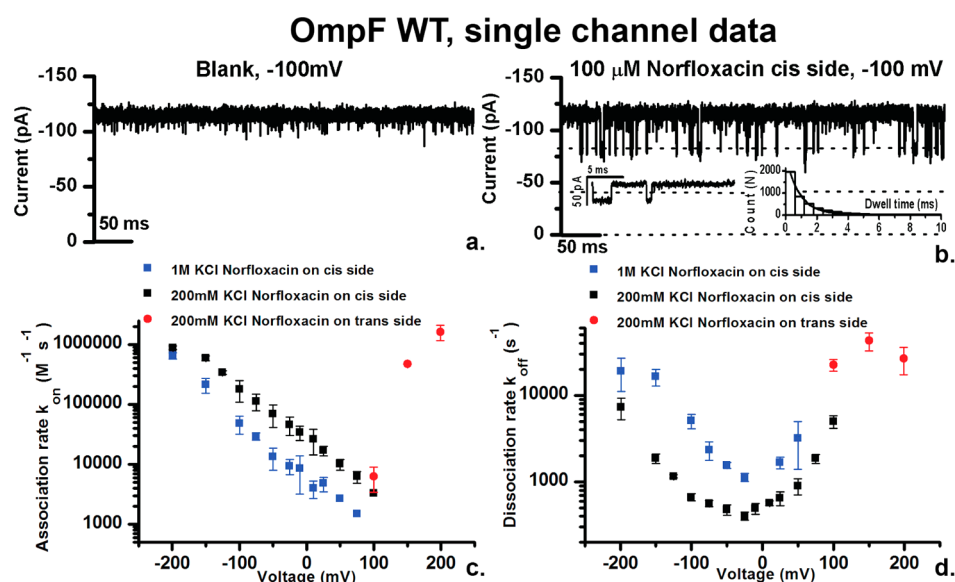
Figure 2. (a) Typical ion current recordings through the single wild-type (WT) OmpF channel in the absence and (b) presence of norfloxacin. (c) Association rates on cis and trans side for OmpF-WT for both 1 M KCl and 200 mM KCl, 5 mM PO_4 pH 7. (d) Dissociation rates at cis and trans for both 1 M KCl and 200 mM KCl, 5 mM PO_4 pH 7 are displayed for (b) OmpF-WT Note that the protein was added always to the cis/ground side.

addition of norfloxacin to the trans side (periplasmic) of the channel causes visibly fewer fluctuations with an average residence time of 50 μs at +100 mV, while no significant events were observed at −100 mV. This asymmetric behavior upon voltage and side of addition, SI, Figure S2, reveals at least two different affinity sites for norfloxacin inside OmpF: a high affinity site (characterized by large residence times; at negative polarity) accessible from the extracellular side (referred as extracellular side 1: ES1) and a low affinity site (characterized by short residence time; at positive polarity) accessible from the periplasmic side (referred as periplasmic side 1: PS1).

The voltage dependence of both the association and the dissociation rates were measured at high and low salt concentration, 1 M KCl and 200 mM KCl, respectively, at pH 7 in the range of −200 to 200 mV. As shown in Figure 2c, an interesting exponential increase of the association rate is observed with increasing negative voltage when the antibiotic is added to the extracellular side, unexpected for a neutral molecule. The dissociation rate increases with increasing applied voltage at both polarities (Figure 2d). At both salt concentrations the trend of voltage dependence is similar, but the association rate and the residence time (reciprocal to the dissociation rate) are higher at 200 mM KCl than at 1 M KCl in the voltage range considered. A stronger interaction at lower salt concentration in both kinetic rates (Figure 2) indicates that the antibiotic interaction with the channel is dominated by electrostatic interactions. At voltages greater than 125 mV (negative polarity) we observed a second type of event with distinguishable shorter relaxation times, referred to as ES2 affinity site, SI, Figures S3 and S4. For such events we do not have a sufficient range to conclude on the voltage dependence, as the bilayer and the pore become unstable above 200 mV.

Activation Enthalpy Calculations. We measured the temperature dependence of the kinetic rate constants for norfloxacin/OmpF-WT in the 200 mM KCl solution from 10 to 35 °C. The exponential dependence of the measured kinetic rate constants for the system (SI, Figure S5a−d) on the applied voltage and on the temperature suggests that the antibiotic

kinetics inside the channel is regulated by a free energy barrier described by a Van't Hoff-Arrhenius type law.[30−32] Therefore, we can define a two-state kinetic model and determine the energy barrier from the electrophysiology data for the entry into the current-blocking binding site (the association barrier), and for the exit from the same site (the dissociation barrier).[27] Following the classical result of the transition-state theory,[27] one may represent the kinetic rates as

$$k = Ae^{-\Delta G^a/k_B T} = Ae^{\Delta S^a/k_B}e^{-\Delta H^a/k_B T} \tag{1}$$

where ΔG^a is the activation free energy, ΔH^a and ΔS^a, are the activation enthalpy, ΔH^a, and entropy, ΔS^a, respectively, and k_B is the Boltzmann constant. In eq 1, the kinetic rate, k, stands for either the association rate constant, k_{on}, or the dissociation rate constant, k_{off} with its corresponding activation free energy, activation entropy, activation enthalpy, and pre-exponential factor, A.

Thus, by using the temperature dependence of the kinetic rate constants, determined in the electrophysiology measurements, it is possible to calculate the corresponding activation enthalpies (Figure 3 and SI, Figure S5) from the slope of the linear fit of ln k vs $1/(k_B T)$.

In the range [−75 mV, +75 mV], the activation enthalpy for dissociation is constant (9 kcal/mol), while the association activation enthalpy linearly depends on the applied voltage:

$$\Delta H_{on}^a = c + \beta V \tag{2}$$

where the coefficients c and $\beta = \partial\, \Delta H_{on}^a/\partial V$ determine the voltage-independent and the voltage-dependent part of the activation enthalpy, respectively, which values are presented in Table 1.

At large negative voltages the linear regime is broken and the association activation enthalpy saturates to the constant value of −10 kcal/mol (Figure 3). In contrast, the activation enthalpy for the dissociation stays within 5 to 10 kcal/mol without any specific trend at higher negative voltages.

Mutagenesis and Validation of Affinity Sites. In order to identify the affinity sites of norfloxacin, we performed
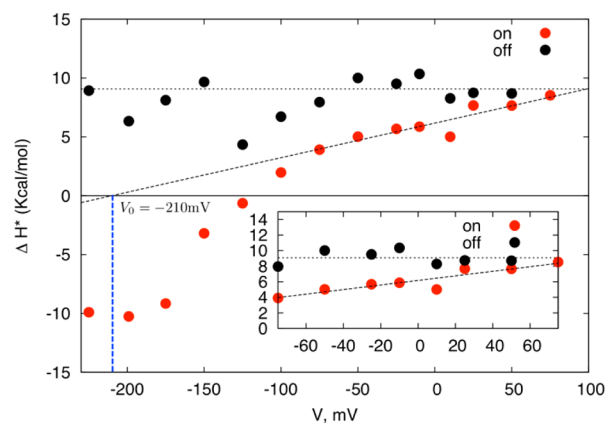
Figure 3. Activation enthalpy for the association (on) and the dissociation (off) rates of norfloxacin in OmpF WT, the linear response regime is highlighted in the inset. Voltage V_0 at which the enthalpy is zero corresponds to the theoretical limit, in the linear regime of eq 1, when the effect of the external electric field on the molecule is compensated by the internal electric field.

Table 1. Results of the Transition State Analysis of the Electrophysiology Data in the Linear Applied Voltage Regime ([−75; +75] mV)[a]

ΔH_{off}^a, kcal/mol	c, kcal/mol	β, kcal/mol/mV	D, debye	h, Å	V_0, mV	E_v mV/Å
9	6	0.03	44	7	−210	30

[a] Activation enthalpy for dissociation, ΔH_{off}^a; the linear fit parameters of the activation enthalpy for association, c and β, respectively the constant and slope; the dipole moment of a norfloxacin molecule, D; the applied voltage corresponding to zero value of the activation enthalpy for association in the linear fit, V_0; the measured transverse electric field in the channel, E_t.

channel mutagenesis in the central region of the pore, R167E/R168E, D121A, D113N, and E117Q, and reconstituted the mutated porins in a planar lipid bilayer. In the double mutant R167E/R168E, the channel exhibits an asymmetric behavior in the association rate, with respect to voltage and side of addition of the antibiotic (Figure 4a). Further, the exponential dependence on applied voltage is maintained. On the other hand, the dissociation constant (Figure 4b and SI, Figure S7) is voltage independent and is enhanced by a factor 40 with respect to the WT, suggesting the involvement of these two residues in the binding process. The same asymmetry, upon addition and voltage, and exponential dependence with respect to applied voltage holds in OmpC WT but with a less steep slope (SI, Figure S8).

The substitution of one of the three acidic residues present in the constricting loop with neutral amino acids destroys the asymmetry upon side addition, as shown in Figure 4c,d and SI, Figure S9 for D113N and SI, Figure S10 for D121A and E117Q. Likewise, the exponential dependence of the association constant disappears for D113N and is weaker for the other two (D121A and E117Q). The dissociation constant for D113N is voltage independent, suggesting the involvement of this residue in the binding site ES1.

Molecular Description with MD Simulations. Starting from the available high-resolution structure of OmpF (PDBID: 2OMF) we used enhanced sampling molecular dynamics simulations (metadynamics) to provide an atomistic view of the interaction of norfloxacin with the channel along the

diffusion path. In previous works,[33,34] two crucial regions for transport along the axis of diffusion (z, Figure 5a) were identified: (i) the preorientation region (PR), (from 5 Å < z < 10 Å; shaded in yellow in Figure 6) with R167, R168, and D121 as key motifs, and (ii) the constriction region (CR) (from 5 Å < z < −5 Å; shaded in purple in Figure 6) which key motifs are the positively charged residues of the basic ladder (R42, R82, R132, K16) and the negatively charged residues of the constricting loop L3 (D113 and E117). These two regions have been previously described as the positive and negative selectivity filters of OmpF.[5] Both regions are characterized by a strong electric field component perpendicular to the axis of diffusion, more intense in the CR than in the PR.[33]

Figure 5b shows the reconstructed free energy surface of the translocation of norfloxacin through OmpF WT without any applied voltage (0 mV) at 1 M KCl salt concentration. A first deep minimum (MD-ES0) is located in the PR (highlighted in green): as it can be observed in (Figure 5e, MD-ES0) norfloxacin interacts with the key motifs of the PR, the two arginines R167/168 and D121 of loop L3, exactly in the same conformation as ampicillin in the cocrystal structure recently obtained by soaking.[35] It is worth to note that ampicillin and norfloxacin, with their charged groups located at the two end sides, share similar shape and electrostatics properties but different flexibility.[8] From this position there are two alternative pathways in the free energy surface, which allow norfloxacin to be transported through the CR of OmpF: it can enter the CR (i) either with its carboxylic group pointing toward the basic ladder (left-side, from 0 to 100 degrees, highlighted red path) (ii) or with its positive (amino) group interacting with the constricting loop (right-side, from 100 to 180 deg, highlighted blue path), toward the MD-ES1 minimum. These two paths are also observed when simulating norfloxacin in OmpF at low salt concentration (SI, Figure S12).

Additional MD experiments were performed for the passage of norfloxacin with an applied potential (−500 mV) at high salt concentration (1 M KCl), for the OmpF-WT (Figure 5c) and for the double mutant OmpF-R167E/R168E (Figure 5d), with norfloxacin added always to the cis side (positive z values) of the pore. In the case of OmpF-WT, as it can be observed in Figure 5c, the applied potential favors the passage through the second pathway (highlighted blue path in Figure 5e, f, and g), characterized by norfloxacin approaching the CR with its positive group toward the constricting loop L3. At high voltages (−500 mV) MD-ES0 is no longer present and a different minimum is found in which the molecule maintains its contact with R167 and R168 (MD-ES2 Figure 5f). From the MD trajectories, it is also noticeable that at high voltage R167 an R168 are oriented toward the CR following the applied field, accompanying the insertion of norfloxacin. The mutation of these two arginines (R167 and R168) with aspartate has strong consequences on the channel-molecule interactions. As shown in Figure 5d and g, the ampicillin-like minimum in the PR is lost because the preorientation transversal electric field is reduced (SI, Figure S13) and the insertion of norfloxacin in the CR with the positive group (blue pathway) is enhanced.

DISCUSSION

Kinetic Model. Combining MD results and mutagenesis data from electrophysiology, we propose a kinetic model for the applied voltage dependence observed (Figure 2c) for norfloxacin association rate. Upon cis addition, electrophysiology experiments suggest the presence of two different
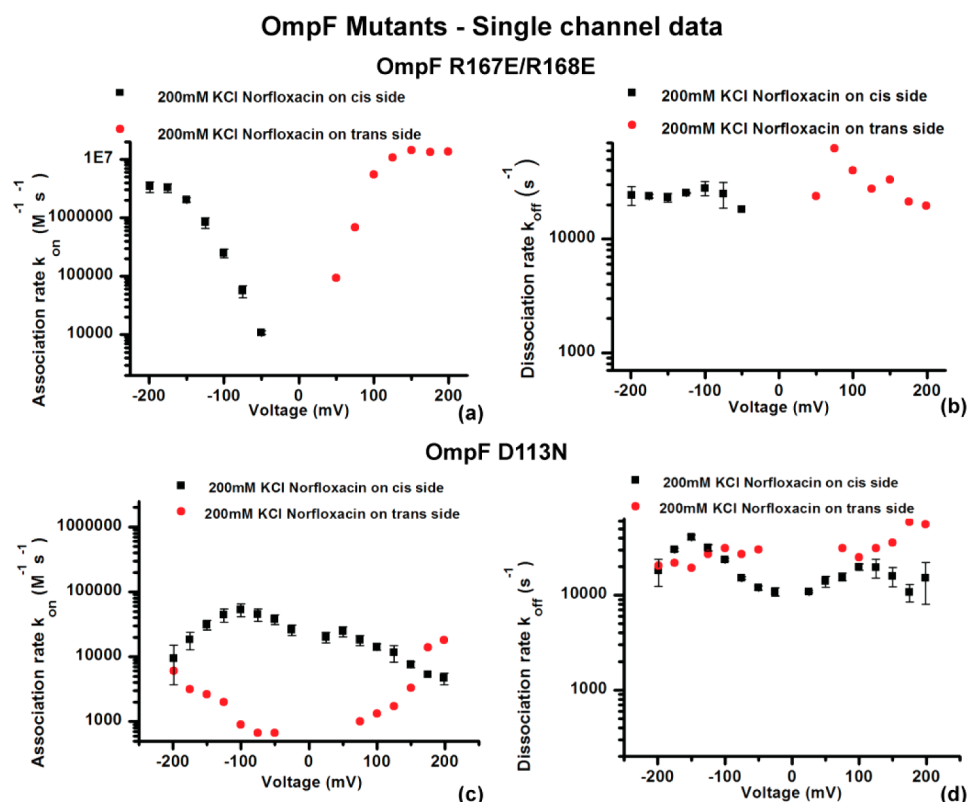
Figure 4. (a) Association rates on cis and trans side for OmpF R167E/R168E for 200 mM KCl, 5 mM PO_4 pH 7. (b) Dissociation rates at cis and trans for OmpF R167E/R168E 200 mM KCl, 5 mM PO_4 pH 7 are displayed. (c) Association rates on cis and trans side for OmpF D113N for 200 mM KCl, 5 mM PO_4 pH 7. (d) Dissociation rates at cis and trans for OmpF D113N 200 mM KCl, 5 mM PO_4 pH 7 are displayed. Note that the protein was added always to the cis/ground side.

affinity sites in which the molecule blocks the current, ES1 and ES2, the latter observed only at high voltages and negative polarity. ES1 corresponds to MD-ES1 (Figure 6) in MD simulations. In this conformation the ionic current of the trimer, calculated from the MD, is decreased by a 30% (2.2 nS with respect to 3.1 nS for the empty trimer, SI, Figure S14, SI, Table S1). ES2 corresponds to MD-ES2 (Figure 5 c,f) in the middle of PR-CR (Figure 6).

In the absence of the applied voltage (Figure 5b,e), before arriving to the high affinity site (MD-ES1/ES1), norfloxacin is aligned in the PR region (MD-ES0, Figure 5b,e) to the internal electric field of the channel[33] (SI, Figure S13), forming an angle of ~55° with the diffusion axis (Figure 6). Due to its size and rigidity norfloxacin cannot enter in the narrow CR in this conformation (MD-ES0). Consequently, it is obliged to reorient and misalign with respect to the internal electric field. This reorientation, from MD-ES0 to MD-ES1, is driven by the selectivity of the CR for positive charges. Thus, the permeation process can be described with a two-step kinetic model: aligning and flipping of the molecule inside the channel (Figure 7).

The addition of a negative external voltage reduces the barrier for norfloxacin reorientation (or flipping) from the MD-ES0 conformation to MD-ES1 (~90° rotation at 0 mV, Figure 6). As norfloxacin is neutral under the chosen measurement conditions, the only direct (linear) interaction between the molecule and the constant applied electric field, E_z, acting along the channel diffusion axis is via its dipole moment projection, D_z. Thus, at small-applied voltages, the voltage dependent part of the activation enthalpy for the association (eq 2) reads:

$$\beta V = -E_z \Delta D_z \tag{3}$$

$\Delta D_z = D_Z^1 - D_Z^0$, is the difference between the molecular dipole moment projection onto the channel axis at the top of the barrier and that in the PR, MD-ES0. This explains the observed linear dependence of the activation enthalpy for association on the applied voltage in the range [−75; +75] mV, Figure 3.

At high voltages the linear regime is no longer valid (Figure 3), and the molecule is aligned by the superimposition of the applied voltage (external electric field) and the intrinsic electric field, leading to the new low affinity MD-ES2/ES2 site (Figure 6) in which norfloxacin forms 130° with the axis of diffusion. This also results in the saturation effect of the activation enthalpy for the association, Figure 3.

Conversely, the activation enthalpy for the dissociation, is voltage independent in the [−75; +75] mV range, Figure 3: norfloxacin in both the MD-ES1/ES1 site and at the top of the barrier is already inside the constriction region and cannot change orientation. The strong voltage dependence of the dissociation rate constant starts at higher voltage and is probably related to the perturbation of the system, and in particular to the formation of binding site MD-ES2/ES2 at negative voltage.

Validation of the Kinetic Model with Mutagenesis Experiments. In the case of the double mutant (OmpF-R167E/R168E), the exponential voltage dependence of the association rate is present but, with a steeper dependence on the applied voltage, suggesting a lower activation barrier to enter in the CR (Figure 4a). The new negative charges reduce the electric field in the PR and induce the molecule to orient
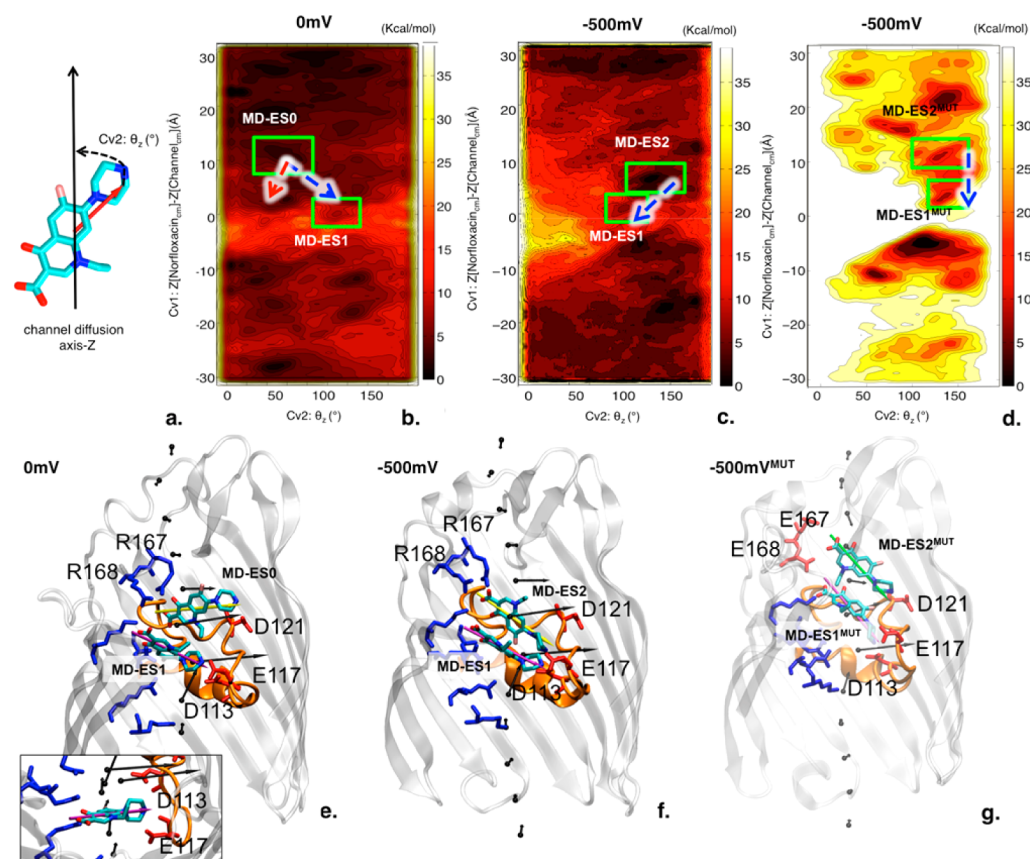
Figure 5. Top: (a) Graphical description of metadynamics collective variables: Cv1 is the position of norfloxacin center of mass (cm) with respect to the cm of the channel along the axis of diffusion (Z) and Cv2 is the orientation angle of the dipole moment of norfloxacin with respect to the axis of diffusion of the channel (Z). (b,c) Reconstructed free energy surfaces for the translocation of norfloxacin through OmpF-WT, respectively, without and with an applied voltage of −500 mV; (d) the same as (c) for OmpF-R167ER168E. Each isocontour corresponds to a free energy difference of 1 kcal/mol, with the absolute minimum equal to zero. Bottom (e,f,g): Cartoon representation of OmpF with norfloxacin affinity poses for the most relevant minima highlighted in green in the corresponding free-energy maps. The loop L3 is highlighted in orange and the intrinsic macroscopic electric field direction is depicted as black arrows. Norfloxacin is represented in licorice and with its electric dipole moment depicted as an arrow. Charged residues are represented in licorice, colored according to the net charge.
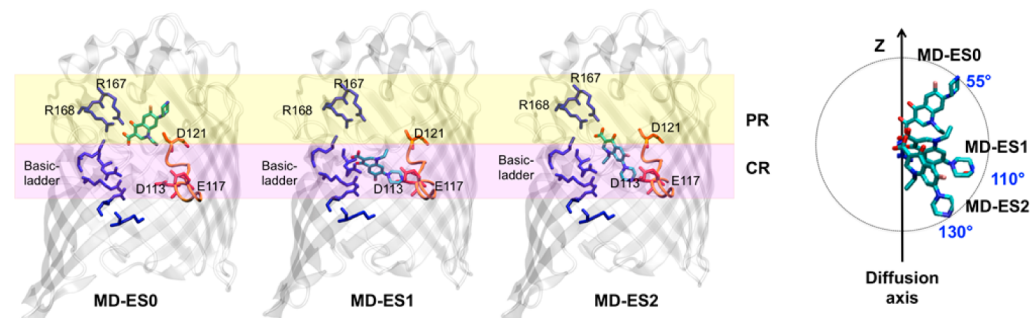

Figure 6. Representation of the three affinity sites of norfloxacin identified with MD simulations: MD-ES0 in the preorientation region (PR), interacting with R167-R168 and D121; MD-ES1 inside the constriction region (CR), interacting with D113-E117 and the basic-ladder; and MD-ES2 in between the two regions, interacting with R167-R168 and D113. For each site norfloxacin pose is represented in licorice as well as the OmpF charged residues, colored according to their net charge and appropriately labeled. The preorientation region is highlighted in yellow and the constriction region in purple. The orientation of the main axis of norfloxacin with respect to the axis of diffusion of the channel is reported on a polar plot for the three affinity sites.

with the positive amino group ahead, already prealigned to enter the binding site, thus decreasing the barrier.

The point mutation on the negative residue of the PR (OmpF-D121A) also affects the initial orientation of norfloxacin. In this case, the molecule orients in the PR with its negative group ahead, requiring a larger reorientation (higher barrier) to enter ES1/MD-ES1 (SI, Figure S10).

If one neutralizes a negative charge in the CR (OmpF-D113N), both the entry and the exit barrier of the molecule are affected, as reflected in the disappearance of the exponential voltage dependence of both the kinetic rates (Figure 4c,d). Because of the lower selectivity (SI, Table S2) and the reduction of electric field (SI, Figure S13), norfloxacin can enter with both orientations guided by the polarity of the
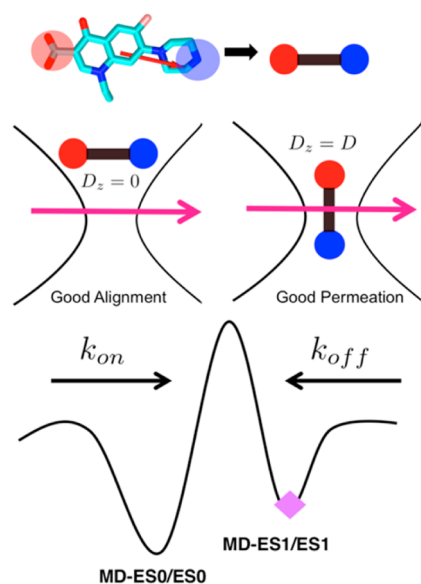
Figure 7. Schematic representation of the kinetic model suggested in this work. From top: norfloxacin seen as a rigid dipole; norfloxacin interacting with the internal electric field near and at the CR; energetics of norfloxacin near (MD-ES0) and at (MD-ES1/ES1) the CR. The purple square indicates the affinity site where the current is blocked.

applied voltage. Further, the disappearance of the exponential voltage dependence of the dissociation rate (Figure 4e), suggests a strong involvement of D113 in the MD-ES1/ES1 affinity site.

There is a good correlation between the selectivity of OmpF/OmpC and their asymmetry in kinetics: the more the channel is selective the higher the asymmetry observed. The sign of voltage that determines the orientation of norfloxacin in all the affinity sites matches the selectivity of the channel for positive charges (SI, Table S2), hence, the molecule has to enter with its positive group facing the CR, either upon cis or trans addition. In the context of drug design our findings might explain why the last generation of β-lactams (cephalosporins, penicillins, and carbapenems) were obtained by adding a positive group increasing susceptibility in Gram-negative bacteria. A similar model can be proposed for ciprofloxacin interaction with OmpF WT (SI, Figure S11), since ciprofloxacin dipolar features are very similar to those of norfloxacin.[22]

Quantification of the Internal Electric Field of the Channel. The suggested interpretation (Figure 7) of the high affinity site, MD-ES1, as the ion-current blocking state (ES1), and the preorientation site, MD-ES0, as the conducting state in the electrophysiology measurements, allows one to determine the key parameters of the interaction between the molecule and our electrostatic nanosieve prototype from the electrophysiology data. If we assume the 90° rotation of the molecule from the preorientation region to the barrier (Figure 7) then in eq 3 we can set $\Delta D_z = D$, where D is the total dipole moment of the norfloxacin. The electric potential (V) is applied to the electrodes immersed into the electrolyte, so that the major potential drop happens in the region of maximum ionic resistance. Taking h as the drop distance around the constriction region of the OmpF channel, we can approximate $E_z = \frac{V}{h}$. As we have assumed that at the activation barrier the main axis of the molecule is aligned with the channel axis,

Figure 7, the potential drop distance can be calculated as $h = \frac{D}{\beta}$. The calculated value of h is presented in Table 1. The value of the potential drop distance (7 Å) is close to the size of the norfloxacin molecule. Therefore, one may conclude that the ions come closely to the molecule, which acts as a cork for ions in the nanopore.

Further, within the linear interaction model, the value of the zero activation enthalpy for association corresponds to the exact compensation of the interaction of the molecular dipole with the internal transversal electric field in the PR region and that with the external field (applied voltage) at the barrier. Therefore, the transversal electric field E_t should be equal to the external one, about 210 mV over 7 Å, or 30 mV/Å (Table 1). This upper value is in very good agreement with the results of the MD simulations (SI, Figure S13) and with the other theoretical[33,36] and experimental values,[37] which predicted an electric field in the range 10−30 mV/ Å inside the OmpF. The use of dipoles that couple with electric field represents an appealing way to manipulate molecules of any size.[38,39]

CONCLUSIONS

We used OmpF as a model pore to understand the electrostatic filtering mechanism of small polar molecules. In the absence of a transmembrane potential, the filtering mechanism is modulated only by the internal electrostatics of the channel, thus acting as an electrostatic nanosieve. We used norfloxacin as a rigid dipolar molecular probe to sense and quantify experimentally the internal electric field inside OmpF. A two-step kinetic model is suggested to describe the molecule pore interaction. Within our model, the dipolar molecule is aligned to the electric field inside the channel in the first step (MD-ES0 conformation) and must be reoriented (MD-ES1 conformation) in order to be transported, due to the size-exclusion effect imposed by the constricted region of the channel (Figure 7). This reorientation or flipping step is affected by the applied voltage and favors the insertion of the positive charged group before, displaying a marked exponential signature in the association rate measured by single-molecule electrophysiology.

Our results show that the central regions of OmpF (PR and CR) ultimately dictates a few basic rules for transport: (i) the charge selectivity of the channel determines which is the chemical group of the molecule penetrating first into the CR, positive in the case of WT-OmpF (ii) the ability of the molecule to rearrange its conformation in order to align its dipole to the intrinsic electric field of the channel and at the same time to fit inside the channel, helps to reduce the steric barrier. According to these rules, a small polar molecule with charged groups, designed so that its dipole moment has a component perpendicular to its main axis, will partially compensate the steric constraint by aligning at the same time its main axis and dipole inside the charge decorated constricted area. The proposed model also shows the importance of using temperature and applied voltage dependent single-channel/single-molecule electrophysiology measurements to extract the key parameters of the molecule-channel interaction.

MATERIALS AND METHODS

Experiments and analysis for bilayer experiments have been performed as described in detail previously.[20] We have used Montal and Muller technique form phospholipid bilayer using DPhPC (Avanti polar lipids).[40] A Teflon cell comprising an aperture of approximately 30−60 μm diameters was placed between the two chambers of the cuvette

(Figure 1a). The aperture was prepainted with 1% hexadecane in hexane for stable bilayer formation. One molar KCl (or 200 mM KCl), 5 mM PO$_4$/10 mM HEPES, pH 7 was used as the electrolyte solution and added to both sides of the chamber. Ion current was detected using standard silver−silver chloride electrodes from WPI (World Precision Instruments) that were placed in each side of the cuvette. Single channel measurements were performed by adding the protein to the cis side of the chamber (side connected to the ground electrode). Spontaneous channel insertion was typically obtained while stirring. After successful single channel reconstitution, the cis side of the chamber was carefully perfused to remove any remaining porins to prevent further channel insertions. Addition of OmpF on one side of the membrane results in asymmetrically distributed orientation recognized by a slight difference in conductance with polarity of voltage. For example: protein addition on the electrically ground side (called cis) results in 11−15% higher conductance at +100 mV compared to −100 mV. Moreover, typical short flickering's are rather observed at −100 mV (SI, Figure S2) ($N > 35$ experiments). We observed preferred (70%) orientation of protein and we assume the extracellular side of protein on cis side. Conductance measurements were performed using an Axopatch 200B amplifier (Molecular Devices) in the voltage clamp mode. Signals were filtered by an on board low pass Bessel filter at 10 kHz and with a sampling frequency set to 50 kHz. Amplitude, probability, and noise analyses were performed using Origin pro 8 (OriginLab) and Clampfit software (Molecular Devices). In a single channel measurement the typical measured quantities were the duration of blocked levels/residence time (τ_c) and the frequency of blockage events (ν). The association rate constant k_{on} was derived using the number of blockage events, $k_{on} = \nu/3[c]$, where c is the concentration of antibiotic. The dissociation rate constant (k_{off}) was determined by averaging the $1/\tau_c$ values recorded over the entire concentration range

MD Simulations. Production run in the NVT ensemble was performed starting from the previously equilibrated OmpF system (PDB CODE 2OMF).[34] After the NVT run, we substituted R167/R168 with E167/E168 to obtain the double mutant, and D113 with N113 for the single mutant. A suitable number of water molecules were replaced with ions to have the desired KCl concentration. All simulations were performed by using the ACEMD code[41] compiled for GPUs, by rescaling hydrogen mass to 4 au and increasing the time-step up to 4.0 fs. The Langevin thermostat was used with 0.1 ps damping time. The Soft Particle Mesh Ewald algorithm was used to treat the electrostatics as for the equilibration stage. The Amber99SB-ILDN force field[42] was used for the protein and lipids, and the TIP3P for waters.[43] The electric field for the OmpF/OmpC and mutants OmpF-R167ER168E, OmpF-D113N were calculated following the method described in ref 33. The GAFF force-field parameters[44] were used to model Norfloxacin as described in ref 33. More details are presented in SI methods.

ASSOCIATED CONTENT

Ⓢ Supporting Information

The Supporting Information is available free of charge on the ACS Publications website at DOI: 10.1021/acsnano.6b08613.

Structure, charge, and dipole of norfloxacin subforms; single channel ion current traces for OmpF/OmpC WT and mutants OmpF R167E/R168E, OmpF D113N, in the presence of norfloxacin; association and dissociation kinetic constants of norfloxacin as a function of voltage in OmpF/OmpC, OmpF-D121A, OmpF-E117Q; single channel ion current traces for OmpF in the presence of ciprofloxacin with association and dissociation kinetic constants as a function of voltage; power spectrum of norfloxacin in OmpF and association/dissociation kinetic constants as a function of temperature; activation enthalpy for association/dissociation of norfloxacin with OmpF as a function of temperature and voltage;

reconstructed free-energy for norfloxacin through OmpF at low ion concentration; internal electric field of OmpF/OmpC and mutants OmpF R167E/R168E, OmpF D113N; calculated ion current for OmpF with and without norfloxacin bound; ion selectivity of all measured channels; calculations for activation enthalpy and details on electric field calculation (PDF)

AUTHOR INFORMATION

Corresponding Author
*E-mail: matteo.ceccarelli@dsf.unica.it; Tel: 39-070-675-4933.

ORCID Ⓒ
Mariano Andrea Scorciapino: 0000-0001-7502-7265
Matteo Ceccarelli: 0000-0003-4272-902X

Author Contributions
[⊥]H.B. and S.A.G. contributed equally to this work. H.B. performed electrophysiology experiments. S.A.G. and G.M. performed modeling of antibiotics and MD simulations. I.B. and H.B. performed analysis and fitting of temperature and voltage electrophysiology data. M.A.S., M.W., and M.C. designed the research. All contributed to writing the manuscript.

Notes
The authors declare no competing financial interest.

REFERENCES

(1) Nikaido, H. Molecular Basis of Bacterial Outer Membrane Permeability Revisited. *Microbiol. Mol. Biol. Rev.* **2003**, *67*, 593−656.

(2) Ujwal, R.; Cascio, D.; Colletier, J.-P.; Faham, S.; Zhang, J.; Toro, L.; Ping, P.; Abramson, J. The Crystal Structure of Mouse VDAC1 at 2.3 A Resolution Reveals Mechanistic Insights into Metabolite Gating. *Proc. Natl. Acad. Sci. U. S. A.* **2008**, *105*, 17742−17747.

(3) Amodeo, G. F.; Scorciapino, M. A.; Messina, A.; De Pinto, V.; Ceccarelli, M. Charged Residues Distribution Modulates Selectivity of the Open State of Human Isoforms of the Voltage Dependent Anion-Selective Channel. *PLoS One* **2014**, *9*, e103879.

(4) van den Berg, B.; Prathyusha Bhamidimarri, S.; Dahyabhai Prajapati, J.; Kleinekathöfer, U.; Winterhalter, M. Outer-Membrane Translocation of Bulky Small Molecules by Passive Diffusion. *Proc. Natl. Acad. Sci. U. S. A.* **2015**, *112*, E2991−E2999.

(5) Miedema, H.; Vrouenraets, M.; Wierenga, J.; Meijberg, W.; Robillard, G.; Eisenberg, B. A Biological Porin Engineered into a Molecular, Nanofluidic Diode. *Nano Lett.* **2007**, *7*, 2886−2891.

(6) Bajaj, H.; Scorciapino, M. A.; Moynié, L.; Page, M. G. P.; Naismith, J. H.; Ceccarelli, M.; Winterhalter, M. Molecular Basis of Filtering Carbapenems by Porins from β-Lactam-Resistant Clinical Strains of *Escherichia Coli*. *J. Biol. Chem.* **2016**, *291*, 2837.

(7) Scorciapino, M. A.; D'Agostino, T.; Acosta-Gutierrez, S.; Malloci, G.; Bodrenko, I.; Ceccarelli, M. Exploiting the Porin Pathway for Polar Compound Delivery into Gram-Negative Bacteria. *Future Med. Chem.* **2016**, *8*, 1047−1062.

(8) Malloci, G.; Vargiu, A. V.; Serra, G.; Bosin, A.; Ruggerone, P.; Ceccarelli, M. A Database of Force-Field Parameters, Dynamics, and Properties of Antimicrobial Compounds. *Molecules* **2015**, *20*, 13997−14021.

(9) de Groot, B. L.; Grubmüller, H. Water Permeation across Biological Membranes: Mechanism and Dynamics of Aquaporin-1 and GlpF. *Science* **2001**, *294*, 2353−2357.

(10) Tajkhorshid, E.; Nollert, P.; Jensen, M. Ø.; Miercke, L. J. W.; O'Connell, J.; Stroud, R. M.; Schulten, K. Control of the Selectivity of the Aquaporin Water Channel Family by Global Orientational Tuning. *Science* **2002**, *296*, 525−530.

(11) Winterhalter, M.; Ceccarelli, M. Physical Methods to Quantify Small Antibiotic Molecules Uptake into Gram-Negative Bacteria. *Eur. J. Pharm. Biopharm.* **2015**, *95*, 63−67.

(12) Tommasi, R.; Brown, D. G.; Walkup, G. K.; Manchester, J. I.; Miller, A. A. ESKAPEing the Labyrinth of Antibacterial Discovery. *Nat. Rev. Drug Discovery* **2015**, *14*, 529−542.

(13) Payne, D. J.; Gwynn, M. N.; Holmes, D. J.; Pompliano, D. L. Drugs for Bad Bugs: Confronting the Challenges of Antibacterial Discovery. *Nat. Rev. Drug Discovery* **2007**, *6*, 29−40.

(14) Stavenger, R. A.; Winterhalter, M. TRANSLOCATION Project: How to Get Good Drugs into Bad Bugs. *Sci. Transl. Med.* **2014**, *6*, 228ed7.

(15) Ghai, I.; Pira, A.; Scorciapino, M. A.; Bodrenko, I.; Benier, L.; Ceccarelli, M.; Winterhalter, M.; Wagner, R. General Method to Determine the Flux of Charged Molecules through Nanopores Applied to β-Lactamase Inhibitors and OmpF. *J. Phys. Chem. Lett.* **2017**, *8*, 1295−1301.

(16) Zhou, Y.; Joubran, C.; Miller-Vedam, L.; Isabella, V.; Nayar, A.; Tentarelli, S.; Miller, A. Thinking Outside the "Bug": A Unique Assay to Measure Intracellular Drug Penetration in Gram-Negative Bacteria. *Anal. Chem.* **2015**, *87*, 3579−3584.

(17) Cama, J.; Bajaj, H.; Pagliara, S.; Maier, T.; Braun, Y.; Winterhalter, M.; Keyser, U. F. Quantification of Fluoroquinolone Uptake through the Outer Membrane Channel OmpF of *Escherichia Coli*. *J. Am. Chem. Soc.* **2015**, *137*, 13836−13843.

(18) Kaščáková, S.; Maigre, L.; Chevalier, J.; Réfrégiers, M.; Pagès, J.-M. Antibiotic Transport in Resistant Bacteria: Synchrotron UV Fluorescence Microscopy to Determine Antibiotic Accumulation with Single Cell Resolution. *PLoS One* **2012**, *7*, e38624.

(19) Mortimer, P. G.; Piddock, L. J. A Comparison of Methods Used for Measuring the Accumulation of Quinolones by Enterobacteriaceae, *Pseudomonas Aeruginosa* and *Staphylococcus Aureus*. *J. Antimicrob. Chemother.* **1991**, *28*, 639−653.

(20) Raj Singh, P.; Ceccarelli, M.; Lovelle, M.; Winterhalter, M.; Mahendran, K. R. Antibiotic Permeation across the OmpF Channel: Modulation of the Affinity Site in the Presence of Magnesium. *J. Phys. Chem. B* **2012**, *116*, 4433−4438.

(21) Wanunu, M. Nanopores: A Journey towards DNA Sequencing. *Phys. Life Rev.* **2012**, *9*, 125−158.

(22) Rodriguez-Larrea, D.; Bayley, H. Multistep Protein Unfolding during Nanopore Translocation. *Nat. Nanotechnol.* **2013**, *8*, 288−295.

(23) Singh, P. R.; Bárcena-Uribarri, I.; Modi, N.; Kleinekathöfer, U.; Benz, R.; Winterhalter, M.; Mahendran, K. R. Pulling Peptides across Nanochannels: Resolving Peptide Binding and Translocation through the Hetero-Oligomeric Channel from Nocardia Farcinica. *ACS Nano* **2012**, *6*, 10699−10707.

(24) Bhamidimarri, S. P.; Prajapati, J. D.; van den Berg, B.; Winterhalter, M.; Kleinekathöfer, U. Role of Electroosmosis in the Permeation of Neutral Molecules: CymA and Cyclodextrin as an Example. *Biophys. J.* **2016**, *110*, 600−611.

(25) van Dorp, S.; Keyser, U. F.; Dekker, N. H.; Dekker, C.; Lemay, S. G. Origin of the Electrophoretic Force on DNA in Solid-State Nanopores. *Nat. Phys.* **2009**, *5*, 347−351.

(26) Gu, L.-Q.; Cheley, S.; Bayley, H. Electroosmotic Enhancement of the Binding of a Neutral Molecule to a Transmembrane Pore. *Proc. Natl. Acad. Sci. U. S. A.* **2003**, *100*, 15498−15503.

(27) Kang, X.-F.; Cheley, S.; Guan, X.; Bayley, H. Stochastic Detection of Enantiomers. *J. Am. Chem. Soc.* **2006**, *128*, 10684−10685.

(28) Danelon, C.; Nestorovich, E. M.; Winterhalter, M.; Ceccarelli, M.; Bezrukov, S. M. Interaction of Zwitterionic Penicillins with the OmpF Channel Facilitates Their Translocation. *Biophys. J.* **2006**, *90*, 1617−1627.

(29) Dhakshnamoorthy, B.; Ziervogel, B. K.; Blachowicz, L.; Roux, B. A Structural Study of Ion Permeation in OmpF Porin from Anomalous X-Ray Diffraction and Molecular Dynamics Simulations. *J. Am. Chem. Soc.* **2013**, *135*, 16561−16568.

(30) Hänggi, P.; Borkovec, M.; Talkner, P. Reaction-Rate Theory: Fifty Years after Kramers. *Rev. Mod. Phys.* **1990**, *62*, 251−341.

(31) Schwarz, G.; Danelon, C.; Winterhalter, M. On Translocation through a Membrane Channel *via* an Internal Binding Site: Kinetics and Voltage Dependence. *Biophys. J.* **2003**, *84*, 2990−2998.

(32) Truhlar, D. G.; Garrett, B. C.; Klippenstein, S. J. Current Status of Transition-State Theory. *J. Phys. Chem.* **1996**, *100*, 12771−12800.

(33) Gutiérrez, S. A.; Bodrenko, I.; Scorciapino, M. A.; Ceccarelli, M. Macroscopic Electric Field inside Water-Filled Biological Nanopores. *Phys. Chem. Chem. Phys.* **2016**, *18*, 8855−8864.

(34) Acosta-Gutierrez, S.; Scorciapino, M. A.; Bodrenko, I.; Ceccarelli, M. Filtering with Electric Field: The Case of *E. Coli* Porins. *J. Phys. Chem. Lett.* **2015**, *6*, 1807−1812.

(35) Ziervogel, B. K.; Roux, B. The Binding of Antibiotics in OmpF Porin. *Structure* **2013**, *21*, 76−87.

(36) Karshikoff, A.; Spassov, V.; Cowan, S. W.; Ladenstein, R.; Schirmer, T. Electrostatic Properties of Two Porin Channels from *Escherichia Coli*. *J. Mol. Biol.* **1994**, *240*, 372−384.

(37) Pfreundschuh, M.; Hensen, U.; Müller, D. J. Quantitative Imaging of the Electrostatic Field and Potential Generated by a Transmembrane Protein Pore at Subnanometer Resolution. *Nano Lett.* **2013**, *13*, 5585−5593.

(38) Merthe, D. J.; Kresin, V. V. Electrostatic Deflection of a Molecular Beam of Massive Neutral Particles: Fully Field-Oriented Polar Molecules within Superfluid Nanodroplets. *J. Phys. Chem. Lett.* **2016**, *7*, 4879−4883.

(39) Freedman, K. J.; Otto, L. M.; Ivanov, A. P.; Barik, A.; Oh, S.-H.; Edel, J. B. Nanopore Sensing at Ultra-Low Concentrations Using Single-Molecule Dielectrophoretic Trapping. *Nat. Commun.* **2016**, *7*, 10217.

(40) Montal, M.; Mueller, P. Formation of Bimolecular Membranes from Lipid Monolayers and a Study of Their Electrical Properties. *Proc. Natl. Acad. Sci. U. S. A.* **1972**, *69*, 3561−3566.

(41) Harvey, M. J.; Giupponi, G.; Fabritiis, G. De. ACEMD: Accelerating Biomolecular Dynamics in the Microsecond Time Scale. *J. Chem. Theory Comput.* **2009**, *5*, 1632−1639.

(42) Lindorff-Larsen, K.; Piana, S.; Palmo, K.; Maragakis, P.; Klepeis, J. L.; Dror, R. O.; Shaw, D. E. Improved Side-Chain Torsion Potentials for the Amber ff99SB Protein Force Field. *Proteins: Struct., Funct., Genet.* **2010**, *78*, 1950−1958.

(43) Jorgensen, W. L.; Chandrasekhar, J.; Madura, J. D.; Impey, R. W.; Klein, M. L. Comparison of Simple Potential Functions for Simulating Liquid Water. *J. Chem. Phys.* **1983**, *79*, 926.

(44) Wang, J.; Wolf, R. M.; Caldwell, J. W.; Kollman, P. A.; Case, D. A. Development and Testing of a General Amber Force Field. *J. Comput. Chem.* **2004**, *25*, 1157−1174.